Gene expression signature-based chemical genomic prediction identifies a novel class of HSP90 pathway modulators

Haley Hieronymus,[1,2] Justin Lamb,[1] Kenneth N. Ross,[1] Xiao P. Peng,[1,3] Cristina Clement,[4] Anna Rodina,[4] Maria Nieto,[5] Jinyan Du,[2] Kimberly Stegmaier,[2] Srilakshmi M. Raj,[1,2] Katherine N. Maloney,[6] Jon Clardy,[6] William C. Hahn,[1,5] Gabriela Chiosis,[4] and Todd R. Golub[1,2,3,*]

[1] The Broad Institute of Harvard University and Massachusetts Institute of Technology, Cambridge, Massachusetts 02142
[2] Department of Pediatric Oncology, Dana-Farber Cancer Institute and Harvard Medical School, Boston, Massachusetts 02115
[3] Howard Hughes Medical Institute, Chevy Chase, Maryland 20815
[4] Department of Medicine and Program in Molecular Pharmacology and Chemistry, Memorial Sloan-Kettering Cancer Center, New York, New York 10021
[5] Department of Medical Oncology, Dana-Farber Cancer Institute and Harvard Medical School, Boston, Massachusetts 02115
[6] Department of Biological Chemistry and Molecular Pharmacology, Harvard Medical School, Boston, Massachusetts 02115
*Correspondence: golub@broad.harvard.edu

Summary

Although androgen receptor (AR)-mediated signaling is central to prostate cancer, the ability to modulate AR signaling states is limited. Here we establish a chemical genomic approach for discovery and target prediction of modulators of cancer phenotypes, as exemplified by AR signaling. We first identify AR activation inhibitors, including a group of structurally related compounds comprising celastrol, gedunin, and derivatives. To develop an in silico approach for target pathway identification, we apply a gene expression-based analysis that classifies HSP90 inhibitors as having similar activity to celastrol and gedunin. Validating this prediction, we demonstrate that celastrol and gedunin inhibit HSP90 activity and HSP90 clients, including AR. Broadly, this work identifies new modes of HSP90 modulation through a gene expression-based strategy.

Introduction

Androgen receptor (AR)-mediated signaling represents a critical pathway in prostate cancer progression (Feldman and Feldman, 2001). Hormonal therapies that reduce circulating androgen levels and inhibit the androgen receptor will initially block prostate cancer growth. Eventually, however, such therapies give rise to fatal drug-resistant, or hormone-refractory, disease. Hormone-refractory prostate cancers commonly show reactivation of AR-mediated signaling through a number of mechanisms (Chen et al., 2004; Feldman and Feldman, 2001; Linja et al., 2001). Androgen-independent tumors often show expression of AR and of AR-induced genes such as PSA. Approximately one- to two-fifths of androgen-independent tumors exhibit increased AR expression after androgen ablation (Linja et al., 2001; Visakorpi et al., 1995), and such AR overexpression appears to allow prostate cancer growth in the face of decreased androgen levels (Chen et al., 2004). Critically, overall expression patterns of androgen-independent tumors are more similar to those of untreated androgen-dependent primary cancers than to those of tumors after neoadjuvant androgen deprivation, suggesting reactivation of AR-mediated transcription (Holzbeierlein et al., 2004).

Though androgen signaling is critical to prostate cancer progression, our ability to modulate AR-mediated signaling programs is limited. Secondary hormonal therapies beyond androgen ablation primarily target ligand-mediated activation of AR, but none appear to be permanently effective against AR signaling-mediated cancer progression (Lam et al., 2006). Additional therapies are in development that may target both AR-mediated signaling and cooperative signaling pathways. Heat shock protein 90 (HSP90) inhibitors, for example, suppress AR signaling and other fundamental oncogenic pathways by promoting degradation of hormone receptors, kinases, and other client proteins (Whitesell and Lindquist, 2005). In general, the current lack of effective AR signaling inhibitors highlights the need for modulators of AR signaling across the full spectrum of AR biology.

Discovery of compounds that modulate complex cancer phenotypes such as androgen independence and signaling

SIGNIFICANCE

Chemical genomics faces the twin challenges of discovering compounds that address complex biological phenotypes and elucidating compounds' targets, once found. Androgen receptor (AR)-mediated signaling that is resistant to existing hormonal therapies represents one such phenotype. Here we apply a generalizable chemical genomic approach for discovering modulators of the AR-mediated signaling program in a prostate cancer cell model of hypersensitive AR signaling. We then develop a gene expression-based method to identify the mechanism of a resulting compound family, using a gene expression compendium of well-characterized drug activities. The utility of this chemical genomic approach is demonstrated by the discovery of two structurally and mechanistically novel modulators of HSP90, a chaperone that stabilizes AR and many other oncogenic proteins.

represents a challenging problem in chemical biology. Gene expression-based chemical discovery has the potential to identify compounds that convert one biological state, as defined by its gene expression signature, to that of a more desirable state without first assaying or identifying each critical effector in the process (Stegmaier et al., 2004). In cancer biology, gene expression-based screening (GE-HTS) allows identification of compounds that revert undesired oncogenic states to those of more nonmalignant or drug-sensitive states. Broadly, gene expression-based chemical discovery represents a strategy for identifying modulators of biological processes with little a priori information about their underlying mechanisms.

An additional problem in chemical biology, perhaps more significant than chemical discovery itself, is the identification of compounds' targets following cell-based discovery (di Bernardo et al., 2005; Gardner et al., 2003). Recent work has applied unbiased gene expression-based approaches to prediction of chemical activity and targets in bacteria and yeast (di Bernardo et al., 2005; Gardner et al., 2003; Parsons et al., 2004). Nonetheless, chemical genomic prediction has not been applied to complex mammalian systems.

Here we illustrate a robust, generalizable approach for chemical genomic discovery and prediction in mammalian cells. Given the limited means available to identify modulators of critical AR signaling pathways and their mechanisms, we set out to discover AR signaling inhibitors using a gene expression signature-based screening approach. Of the hits that emerged, celastrol and gedunin compounds represent a structurally similar group of natural products with a history of medicinal and anticancer use. To investigate the target activity of these compounds, we used an approach to connect the activities of celastrol and gedunin to drugs with known biological activities at the gene expression level, using a compendium of gene expression profiles of drug treatment. Celastrol and gedunin both invoked gene expression signatures highly similar to those of existing HSP90 inhibitors. Subsequent work validated this gene expression-based activity prediction. However, celastrol and gedunin do not act directly on the HSP90 ATP-binding pocket, unlike most existing HSP90 inhibitors. Instead, they act synergistically with existing HSP90 inhibitors to suppress HSP90 client signaling and viability. In all, we demonstrate the discovery of HSP90 functional inhibition through a generalizable gene expression-based approach for compound discovery and elucidation.

Results

Gene expression-based screen identifies inhibitors of AR activation signature

Because of the paucity of effective AR-mediated signaling inhibitors, we set out to identify new inhibitors of AR activation using a gene expression signature-based screening approach (Stegmaier et al., 2004). GE-HTS identifies compounds that convert a gene expression signature representing one state to that of another, using a high-throughput bead-based method to quantify the gene expression signatures (Figure 1A; Peck et al., 2006). Here, we asked whether GE-HTS could be used to identify androgen signaling modulators that revert the signature of the androgen-activated state to the signature of the quiescent, androgen-deprived state in prostate cancer cells.

Toward that end, we first defined the gene expression signature of AR activation in the LNCaP prostate cancer cell line, a common in vitro model of AR-mediated signaling in prostate cancer (Chen et al., 2004). The signature was defined by identifying genes that are activated or repressed by androgen stimulation (0.1 nM R1881, 24 hr) relative to androgen deprivation, using microarray-based gene expression profiling (Febbo et al., 2005). The AR activation signature was refined to 27 genes that showed robust activation or inhibition of expression upon androgen stimulation as measured in our GE-HTS bead-based assay (Figure 1B). The final 27 gene signature therefore represents a gene set that associates with androgen signaling at a selected level of robustness.

Next, we asked whether the multigene GE-HTS approach provides significant advantages over conventional screening approaches for androgen signaling inhibitors. We found that the GE-HTS method performed better than a single reporter assay due to the robustness provided by a multigene readout. Compared to a single-gene readout using the best marker gene in the microarray data, the 27 gene signature decreased the false-positive rate of our screen 14-fold and the false-negative rate 7-fold, as determined by leave-one-out crossvalidation using weighted voting and K-nearest neighbors analysis (Table S5 in the Supplemental Data available with this article online). Further, GE-HTS allows the assay of endogenous AR-mediated gene induction and repression, rather than expression in a non-chromatin reporter system.

GE-HTS screening was then carried out for compounds that convert the AR activation signature to the androgen-deprived signature. Compound libraries comprising approximately 2500 compounds and enriched in drugs and natural products were screened. LNCaP cells were treated for 24 hr with synthetic androgen R1881 and compound for the GE-HTS screen. In parallel, the libraries were screened for their effects on LNCaP viability over 3 days using a luminescent ATP quantitation assay.

The screen identified more than 20 compounds that robustly suppress the androgen signaling signature without causing severe toxicity in vitro, while another 30 were found to mildly inhibit the signature (Table S1; Figures S1 and S2). Compounds that inhibit the androgen signaling signature were identified using three analytic metrics: summed gene expression, K-nearest neighbors, and naive Bayes classification. These metrics incorporate both supervised and unsupervised approaches as well as parametric and nonparametric statistics. Strong hits were defined as compounds that induced the androgen deprivation signature in at least two of three replicates by all three measures at $p < 0.05$. Weak hits were defined as compounds that induced the androgen deprivation signature in at least two of three replicates by only two measures ($p < 0.05$). These hits were subsequently filtered to remove compounds that inhibited cell growth by more than 50% over 3 days.

Many of the identified androgen signaling signature inhibitors have provocative activities. They include prazosin, a drug currently used for treatment of benign prostatic hyperplasia (Walsh, 1996), and the mTOR inhibitor rapamycin, which is currently in clinical trials as a treatment for advanced prostate cancer (Majumder and Sellers, 2005). Dexamethasone acetate was also found to strongly inhibit the androgen signaling signature, and a range of other glucocorticoids were identified as weak inhibitors; glucocorticoids are currently used for their systemic effects in prostate cancer treatment but may also have a direct effect on prostate cancer cell signaling (Lam et al., 2006). Most notably, a large set of celastrol and gedunin natural products

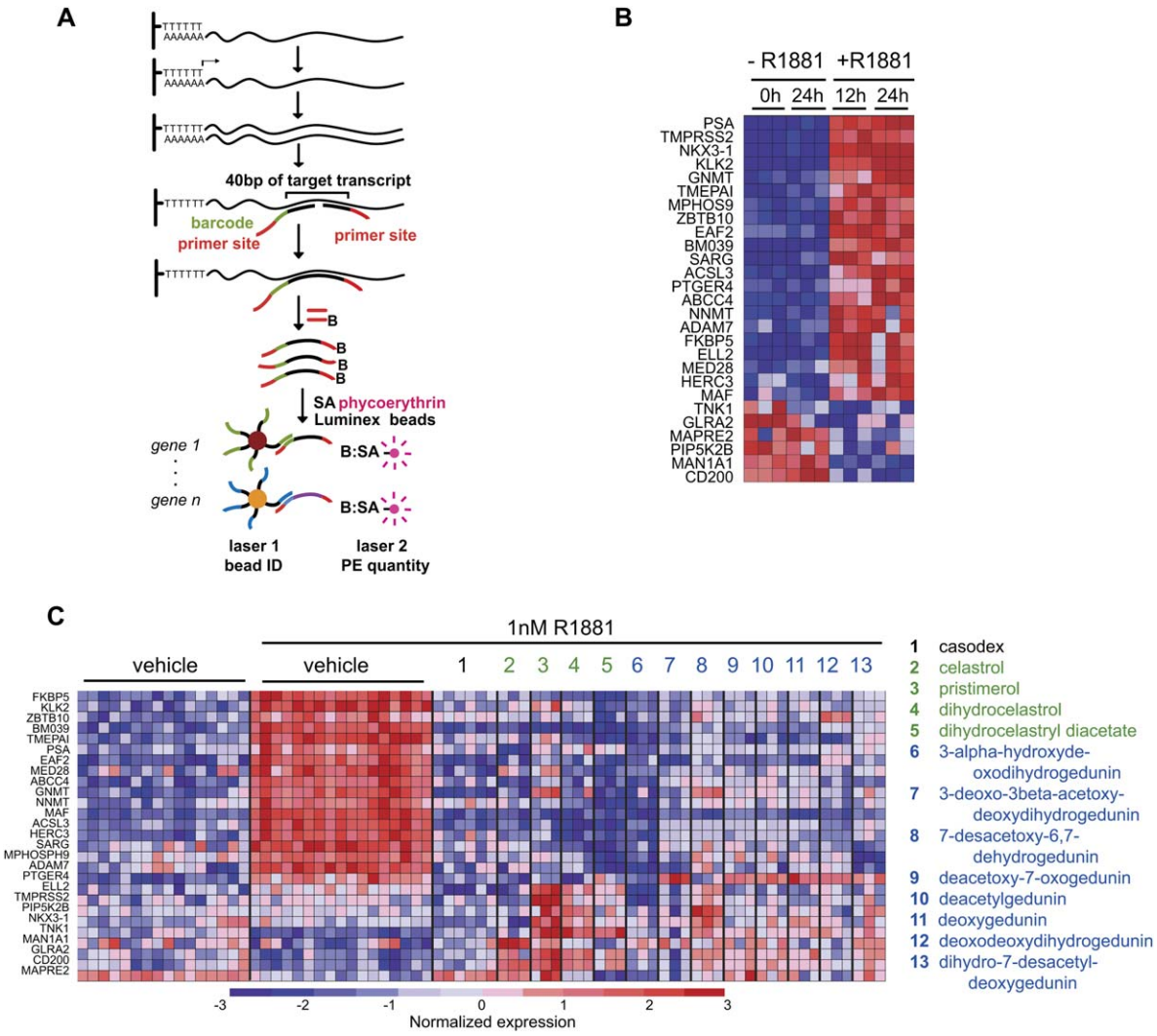

Figure 1. Gene expression-based screen identifies inhibitors of androgen signaling signature

A: A high-throughput method for quantifying transcript levels was developed to enable gene expression signature-based screens. In this method, mRNA in cell lysates is hybridized to dT_{20}-conjugated plates and then reverse transcribed. The resulting covalently attached cDNA is amplified by ligation-mediated PCR. For each gene to be assayed, ligation generates a sequence complementary to the transcript and flanked by a unique barcode tag and universal primer sites. The ligation product is PCR amplified using biotin-conjugated universal primers. The PCR products are then captured by hybridization to probes complementary to the barcodes that are attached to uniquely colored polystyrene beads. The products are subsequently stained with streptavidin-phycoerythrin (SAPE). Each gene product is identified by the color of its capture bead and quantified using the associated SAPE fluorescence, as measured by two-laser flow cytometry.

B: A gene expression signature of androgen stimulation was defined from gene expression profiles of LNCaP cells stimulated with the synthetic androgen R1881 for 12 hr and 24 hr, as compared to androgen-deprived LNCaP cells. The 27 gene signature contains both androgen-induced and androgen-repressed genes, shown here by row-normalized heat map.

C: GE-HTS screen identifies a family of celastrol and gedunin compounds that revert the androgen signaling signature to the androgen-deprived signature in LNCaP cells. LNCaP cells were treated with 1 nM R1881 plus compounds at ~20 μM for 24 hr. The heat map shows the row-normalized signatures induced by gedunin and celastrol compounds in the screen and the competitive AR inhibitor casodex (bicalutamide).

made up more than a quarter of the identified AR signaling inhibitors (Figure 1C), and these compounds were therefore studied in greater detail.

Celastrol, gedunin, and derivatives represent a structurally similar group of natural products that inhibit androgen signaling

The celastrol and gedunin triterpenoids represent a dominant family of structurally similar compounds that emerged from our GE-HTS screen (Figures 1C and 2A). Celastrol and six gedunin derivatives showed strong inhibition of the androgen signaling signature (Figure 1C), while two gedunin derivatives and three celastrol derivatives also showed weak inhibitory activity (Table S1). Celastrol and gedunin are natural products derived from plants of the *Celastracae* and *Meliacae* families that have been used therapeutically for several millennia, though little is known about their cellular targets (Padma, 2005; Ushiro et al., 1997). Celastrol and gedunin compounds show structural similarity (Figure 2A; Figures S1A and S2A). Moreover, celastrol and gedunin invoked similar global gene expression changes,

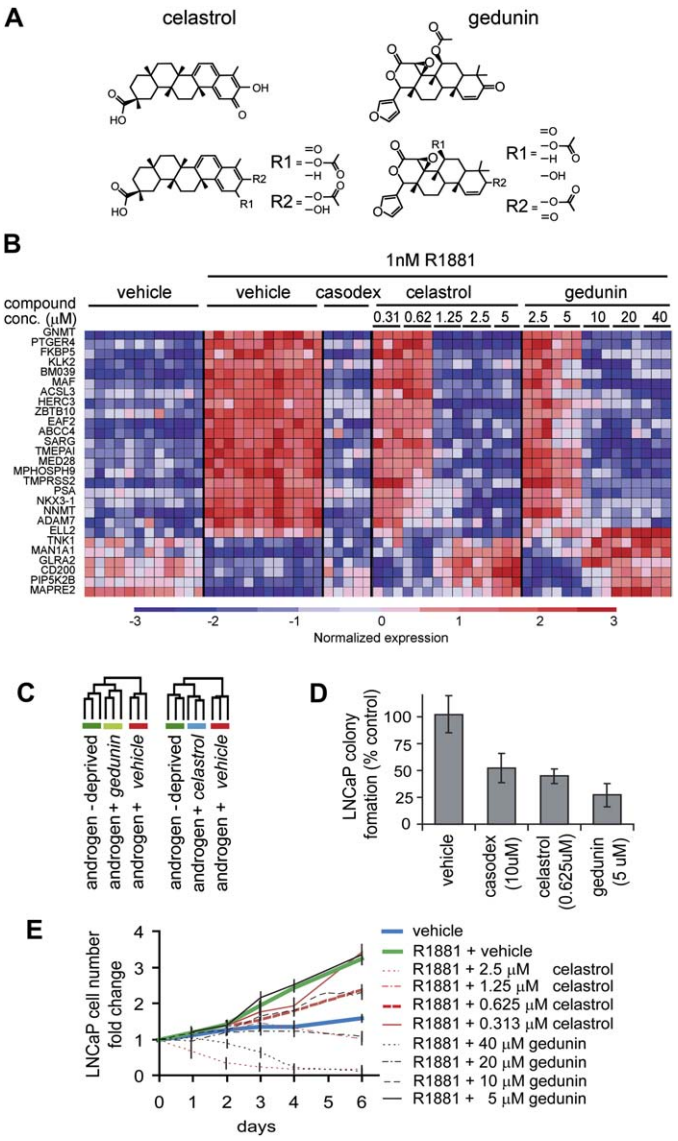

Figure 2. Celastrol and gedunin inhibit androgen signaling

A: Structures of celastrol and gedunin are shown (top). Derivatives of celastrol (left, bottom) and gedunin (right, bottom) identified as AR signature inhibitors by GE-HTS are also shown.

B: Celastrol and gedunin inhibit the GE-HTS androgen signaling signature in a concentration-dependent manner. LNCaP cells were treated with 1 nM R1881 for 12 hr and then 1 nM R1881 plus compound for an additional 24 hr. Controls were treated with vehicle in place of R1881 and/or compound. The row-normalized GE-HTS signature shows concentration-dependent reversion to the androgen deprivation signature.

C: Celastrol- and gedunin-mediated effects on androgen-responsive gene expression mimics androgen deprivation. Average link hierarchical clustering was carried out on androgen-responsive gene expression from androgen-deprived cells (green) and androgen-treated cells with vehicle (red), celastrol (1.25 μM, 24 hr, blue), or gedunin (20 μM, 24 hr, yellow). The dendrograms show the clustering of the samples within the androgen-responsive gene space.

D: Celastrol and gedunin inhibit anchorage-independent prostate cancer cell growth. Celastrol and gedunin inhibit LNCaP colony formation in soft agar (mean of three replicates ± 1 SD).

E: Celastrol and gedunin inhibit adherent prostate cancer cell growth. Celastrol (red) and gedunin (black) inhibit growth of LNCaP cells, as determined by luminescent assay of ATP level (mean of four replicates ± 1 SD).

when we assayed the gene expression effects of celastrol (1.25 μM, 6 hr) and gedunin (20 μM, 6 hr) by genome-wide DNA microarray. The genes regulated by celastrol and gedunin were highly overlapping ($p < 10^{-18}$, Fisher's exact test; see Supplemental Data). Celastrol, gedunin, and their derivatives therefore represent a family of AR signaling inhibitors with similar structure and activity at the gene expression level.

To validate the effect of celastrol and gedunin on AR-mediated signaling, we first established that they inhibit the GE-HTS androgen signaling signature in a concentration-dependent manner in LNCaP cells (Figure 2B). Because natural products often contain impurities, we verified that celastrol and gedunin used for this work were >98% and >99% pure, respectively, by HPLC and NMR. Celastrol- and gedunin-induced inhibition was seen both with and without 12 hr pretreatment with androgen (Figure 2B and data not shown). Celastrol and gedunin therefore inhibit the androgen signaling signature outside the screen context.

We next asked whether celastrol and gedunin inhibit the broader program of androgen signaling beyond the GE-HTS signature. To address this question, we compared the genome-wide gene expression profiles of androgen-stimulated LNCaP cells treated with celastrol (1.25 μM) and gedunin (20 μM) for 24 hr to those of androgen-stimulated and androgen-deprived cells. Hierarchical clustering indicated that androgen-responsive gene expression (Febbo et al., 2005) of compound-treated androgen-stimulated cells is more similar to that of androgen-deprived cells than to that of vehicle-treated androgen-stimulated cells (Figure 2C). Celastrol and gedunin treatment therefore invoked a broader gene expression program similar to that induced by androgen deprivation, though differences between them can still be seen.

To investigate the cellular consequences of celastrol- and gedunin-mediated inhibition, we assessed whether celastrol and gedunin activity results in decreased cell growth, consistent with AR inhibition. First, we determined whether the compounds inhibit adherent growth of androgen-stimulated LNCaP cells by luminescent assay of ATP levels. The compounds mimic the growth-inhibitory effects of androgen deprivation around the EC_{50} of androgen signaling inhibition (Figures 2D and 2E). Second, the compounds' effects on anchorage-independent growth of LNCaP cells was assayed in soft agar (Figure 2D). Celastrol (0.625 μM) and gedunin inhibited anchorage-independent growth to a similar degree as the AR competitive antagonist bicalutamide (casodex). In addition to reducing colony number, celastrol and gedunin inhibited colony size (data not shown). Celastrol and gedunin therefore inhibit adherent and anchorage-independent growth of LNCaP cells, likely, in part, due to suppression of AR signaling.

Gene expression compendium of drug effects identifies HSP90-inhibitory activity of celastrol and gedunin

While celastrol and gedunin clearly inhibit AR-mediated signaling, their target and mechanism are not obvious. Indeed, a major challenge in cell-based chemical biology and chemical genomics is the identification of compounds' targets (Gardner et al., 2003). We hypothesized that gene expression signatures could be used to identify compound action based on the similarity of such compound-induced signatures to signatures of existing drugs of known mechanism. We therefore employed a collection of gene expression profiles of drug-treated cell lines

that was developed in our lab, termed the Connectivity Map (Lamb et al., 2006). This database comprises 453 genome-wide Affymetrix expression profiles derived from the treatment of human cell lines with 164 small molecules, primarily FDA-approved drugs. A 6 hr treatment time was chosen in an attempt to capture the primary, and potentially mechanistic, effects of the compounds rather than the downstream phenotypic consequences.

In order to use the Connectivity Map to gain insight into celastrol and gedunin function, we first defined a gene expression signature of celastrol and gedunin activity. The expression signatures of celastrol and gedunin were derived by expression profiling of RNA from LNCaP cells treated with celastrol (1.25 μM), gedunin (20 μM), and vehicle (DMSO) for 6 hr; signatures were defined using comparative marker selection to identify transcripts that distinguished between the compound- and vehicle-treated profiles by the signal-to-noise (SNR) metric. The enrichment of these signatures in the gene expression profiles of the Connectivity Map database was then assessed using a gene enrichment metric, the connectivity score, based on the Kolmogorov-Smirnov statistic (Lamb et al., 2003). Out of 164 compounds represented by the Connectivity Map, celastrol was the top match for the gedunin signature and the fourth-ranked match for the celastrol signature (Table S2). The enrichment of the LNCaP celastrol signature in the MCF7 celastrol gene expression profile validates our ability to identify true similarities using the Connectivity Map and their cell line independence. Moreover, the enrichment of the gedunin signature in the celastrol profile demonstrates similarity between celastrol and gedunin activities.

To generate hypotheses regarding celastrol and gedunin targets, the Connectivity Map was used to identify known drugs with highly similar gene expression effects. The celastrol and gedunin signatures showed very strong similarity to the gene expression profiles of four HSP90 inhibitors: geldanamycin (n = 6), 17-dimethylaminoethylamino-17-demethoxy-geldanamycin (17-DMAG; n = 2), 7-allylamino-17-demethoxygeldanamycin (17-AAG; n = 18), and monorden (radicicol; n = 10) (Figure 3A; Table S2). Geldanamycin and its derivatives induced gene expression profiles that were highly enriched with celastrol and gedunin signature genes at 6 hr, as shown by the high enrichment score ranking of these compounds relative to other compounds in the Connectivity Map database (Figure 3A). For example, celastrol- and gedunin-induced genes were enriched in the 17-AAG profile (Figure 3B, green), whereas celastrol- and gedunin-repressed genes were similarly repressed by 17-AAG (Figure 3B, red). In contrast, a signature of randomly selected genes did not show enrichment over this 17-AAG profile (Figure 3B). The radicicol profiles were similarly enriched, albeit to a lesser extent (data not shown). The similarity of celastrol and gedunin activities to HSP90 inhibition is supported by the significant number of replicates (Figure 3A, single instances) and the number of different HSP90 inhibitors (Figure 3A, combined instances) that show this enrichment. The signatures of 24 hr celastrol and gedunin treatment also showed similarity to the HSP90 inhibitor profiles, though to a somewhat lesser degree (data not shown). HSP90 inhibition therefore represents a major gene expression signature invoked by celastrol and gedunin. More generally, this work illustrates a robust approach for using gene expression signatures to gain insight into chemical activity.

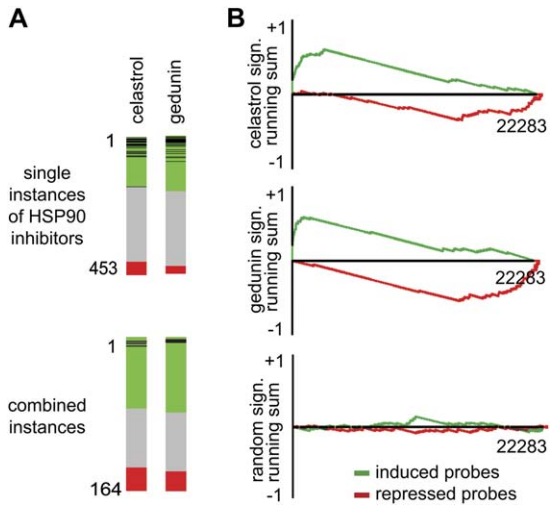

Figure 3. Gene expression compendium of drug treatment predicts HSP90-inhibitory activity of celastrol and gedunin

A: Celastrol and gedunin gene expression signatures are similar to the gene expression profiles of HSP90 inhibition. From a collection of gene expression profiles representing 164 compounds, the expression profiles of 17-AAG, 17-DMAG, and geldanamycin treatment (6 hr, MCF7) show enrichment of celastrol (1.25 μM, 6 hr, LNCaP) and gedunin (20 μM, 6 hr, LNCaP cells) signatures at 6 hr. The barview is constructed from 453 horizontal lines, each representing an individual treatment instance and ordered by their corresponding enrichment with the celastrol and gedunin query signatures. All geldanamycin (n = 6), 17-allylamino-geldanamycin (n = 18), and 17-dimethylamino-geldanamycin (n = 2) instances are colored in black. Colors applied to the remaining instances reflect positive (green), negative (red), or no (gray) enrichment with the celastrol and gedunin query signatures. The combined barview is constructed from horizontal lines, each representing a compound treatment and ordered as for the single instance barview. **B:** Enrichment of the celastrol and gedunin signatures in a selected 17-AAG instance. Celastrol and gedunin induce (green) and repress (red) gene probes that are enriched in the 17-AAG gene expression profile (22,283 probe sets), ordered by their extent of differential expression between treatment and control scans for the 17-AAG instance (x axis). The Kolmogorov-Smirnov score is shown for the induced and repressed signatures of celastrol (1.25 μM, 6 hr, LNCaP) and gedunin (20 μM, 6 hr, LNCaP) across the best matched 17-AAG gene expression profile (1 μM, 6 hr, MCF7). The fact that most celastrol- and gedunin-induced genes appear early in the ordered 17-AAG profile and are therefore enriched in the 17-AAG-induced signature is illustrated by this graphical representation of the Kolmogorov-Smirnov analysis (green). The converse is true for the repressed genes (red). A signature populated with randomly selected probe sets shows no enrichment.

Celastrol and gedunin inhibit the HSP90 pathway

Having used the Connectivity Map to generate the hypothesis that celastrol and gedunin function as HSP90 inhibitors, we next sought to validate this hypothesis. Since AR is an HSP90 client protein, celastrol- and gedunin-mediated inhibition of HSP90 could explain the observed suppression of androgen signaling. HSP90 inhibition induces degradation of AR and other client proteins and thereby targets multiple, cooperative oncogenic signaling pathways.

We first asked whether celastrol and gedunin decrease the levels of AR itself. Both celastrol and gedunin were found to decrease AR protein levels in a concentration-dependent manner (Figure 4A). Celastrol decreased AR levels in LNCaP cells at 0.5 μM and above, while gedunin decreases their levels at 10 μM and above. Almost complete ablation of AR levels was seen at 1 μM celastrol and 20 μM gedunin. These concentration-dependent effects on AR are consistent with the observed

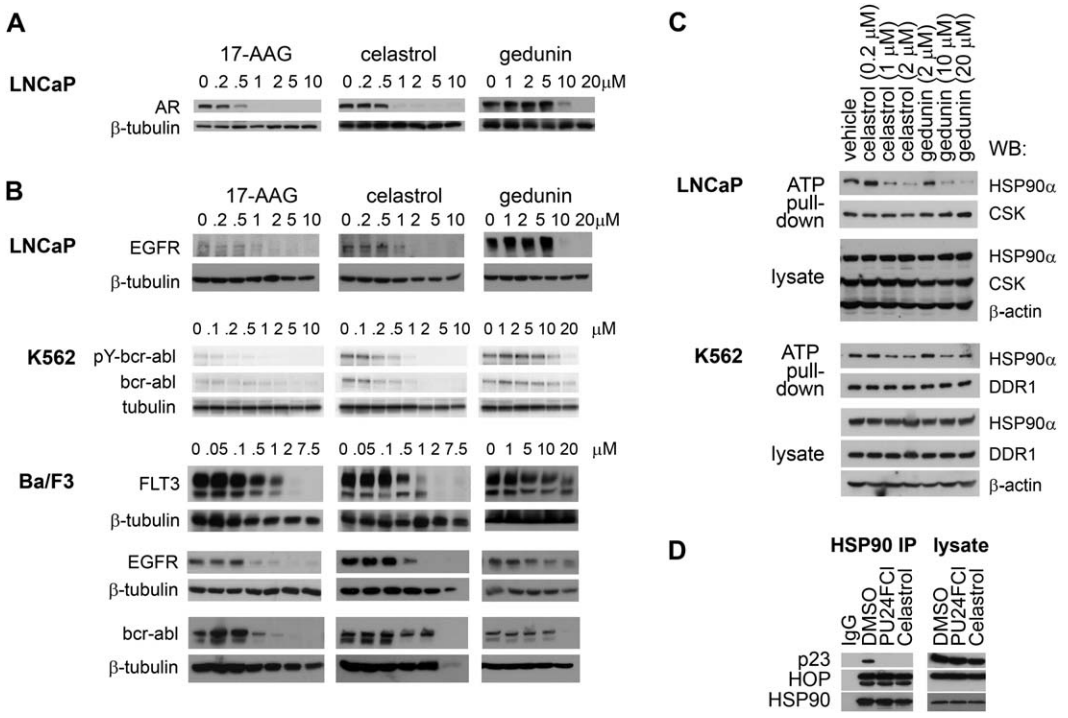

Figure 4. Celastrol and gedunin inhibit the HSP90 pathway

A: Celastrol and gedunin lower HSP90 client protein levels. Celastrol and gedunin induce concentration-dependent decreases in AR level at 24 hr. 17-AAG treatment is shown as a positive control.

B: Celastrol and gedunin decrease the levels of HSP90 clients BCR-ABL1, EGFR, and FLT3. Celastrol and gedunin treatment for 24 hr lowers EGFR levels in LNCaP cells, BCR-ABL1 levels, and phosphorylation in K562 cells, and FLT3, EGFR, and BCR-ABL1 levels in Ba/F3 cells. Ba/F3 cells overexpressing BCR-ABL1 were particularly susceptible to death upon celastrol treatment, resulting in lowered total protein level at 7.5 μM celastrol.

C: Cellular treatment with celastrol and gedunin inhibits HSP90 ATP-binding activity. HSP90 from lysates of celastrol- or gedunin-treated LNCaP and K562 cells show decreased binding to ATP-polystyrene relative to vehicle-treated cells. ATP-binding proteins were isolated from treated LNCaP and K562 cells by ATP affinity purification and detected by western blot. Affinity-purified proteins (pulldown) and total lysate were blotted for HSP90α, control ATP-binding proteins CSK (LNCaP), DDR1 (K562), and actin.

D: Celastrol decreases HSP90 interaction with its cochaperone p23. Celastrol treatment of SKBR-3 cells (2.5 μM, 12 hr) decreased the amount of p23 that coimmunoprecipitated with HSP90, as shown by western blot of the coimmunoprecipitate and lysate. Celastrol did not affect the amount of coimmunoprecipitating HOP, shown as a control. The C-terminal HSP90 inhibitor PU24FCl (20 μM, 24 hr) is shown as a control.

inhibitory effects on AR-mediated signaling. Notably, HSP90 inhibitors 17-AAG and geldanamycin suppressed the androgen signaling signature as well (data not shown).

To more broadly establish the effects of celastrol and gedunin on the HSP90 pathway, we tested whether these compounds decrease the protein levels of other HSP90 clients. Celastrol and gedunin treatment lowered the protein levels of FLT3, EGFR, and BCR-ABL1 in a concentration-dependent manner in several cell lines (Figure 4B). These findings demonstrate that celastrol and gedunin decrease the levels of a range of HSP90 client proteins.

Given their inhibition of HSP90 clients, we next asked whether celastrol and gedunin affect HSP90 activity itself. To assess the effects on HSP90 activity within a cellular context, we treated LNCaP and K562 cells with celastrol or gedunin for 24 hr and subsequently tested the cellular HSP90's ATP-binding activity. ATP-binding activity was assayed by ATP-polyacrylamide pulldown of HSP90 from cell lysates, followed by western blot-based quantification (Bali et al., 2005). This assay identifies HSP90 inhibition, both direct and indirect, that alters HSP90 ATP-binding activity in cell lines (Bali et al., 2005; Soti et al., 2002). We found that celastrol and gedunin treatment inhibited the ATP-binding activity of HSP90α in both cell lines (Figure 4C). In contrast, compound treatment did not affect the ATP-binding activity of the kinases CSK and DDR1, which are not HSP90 clients. The decrease in ATP binding by HSP90 cannot be accounted for by changes in HSP90 level (Figure 4C). Celastrol and gedunin therefore inhibit HSP90 activity itself in a cellular context, either directly or indirectly.

Celastrol, as the more potent compound, was then tested for effects on HSP90's functional interactions with cochaperones. Consistent with its reduction of HSP90 ATP-binding activity, celastrol treatment reduced HSP90 interaction with the cochaperone p23 in SKBR-3 cells, as determined by coimmunoprecipitation with HSP90 (Figure 4D). The N-terminal inhibitor PU-H71 (He et al., 2006; Vilenchik et al., 2004) had the same effect. p23 interacts with the ATP-bound form of HSP90 and helps stabilize the mature steroid receptor-HSP90 complex (Felts and Toft, 2003). Geldanamycin and other HSP90 inhibitors are known to inhibit p23 association with HSP90 (Felts and Toft, 2003). In contrast, HSP90-HOP interaction was unaltered by celastrol and other HSP90 inhibitors (Figure 4D). Thus, celastrol inhibits the functional interactions of HSP90 and suppresses HSP90 client levels.

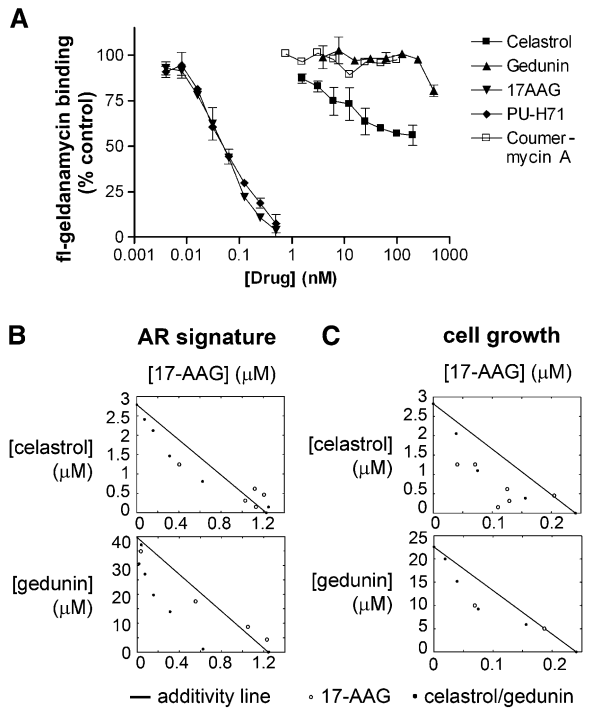

Figure 5. Celastrol and gedunin inhibit HSP90 function through a different mechanism than existing HSP90 ATP-binding pocket inhibitors

A: Celastrol (black squares) and gedunin (black upward triangles) do not compete with Cy3B-labeled geldanamycin for binding to the ATP-binding site of HSP90α in vitro at pharmacological doses, unlike N-terminal inhibitors 17-AAG (black downward triangles) and PU-H71 (black diamonds). The decrease in fluorescence polarization of Cy3B-geldanamycin upon displacement from the ATP-binding pocket of recombinant hHSP90α is shown. The novobiocin-analog coumermycin A (white squares) is shown as a C-terminal binding control. The mean ± 1 SD is shown.

B: Celastrol and gedunin show synergistic inhibition of AR signaling with the HSP90 inhibitor 17-AAG. The combined effect of these compounds and 17-AAG on the LNCaP androgen signaling signature at 24 hr is shown by isobologram. Synergy appears as points below the line of additivity.

C: Celastrol and gedunin show synergistic growth inhibition with 17-AAG. The combined effect of these compounds and 17-AAG on LNCaP cell viability at 24 hr, as determined by ATP level, is shown by isobologram.

Celastrol and gedunin modulate HSP90 activity by a mechanism that is distinct from that of existing HSP90 ATP-binding pocket inhibitors

Since celastrol and gedunin inhibit HSP90 pathway function, we asked whether celastrol and gedunin act by competitively binding to the ATP-binding pocket of HSP90, the mechanism common to most HSP90 inhibitors (Whitesell and Lindquist, 2005). We first tested whether celastrol or gedunin could compete with Cy3B-geldanamycin for binding to the ATP-binding pocket of purified HSP90α by fluorescence polarization assay (Kim et al., 2004; Llauger-Bufi et al., 2003). In contrast to the earlier ATP-binding activity assay, this experiment tested the ability of celastrol and gedunin to directly inhibit small molecule binding to the ATP pocket of purified HSP90 when combined in vitro. Neither celastrol nor gedunin significantly competed with geldanamycin binding to recombinant HSP90α at concentrations up to ~100 μM, with compound addition before and after geldanamycin addition (Figure 5A). The N-terminal inhibitors 17-AAG and PU-H71, on the other hand, competed with geldanamycin binding at low concentrations in vitro (Figure 5A) (He et al., 2006; Vilenchik et al., 2004). These results indicate that celastrol and gedunin act on HSP90 by a different mechanism than existing N-terminal HSP90 inhibitors.

If celastrol and gedunin act on HSP90 function via a distinct mechanism from HSP90 ATP-binding site inhibition (Bagatell et al., 2005), they might act synergistically with existing HSP90 inhibitors. We therefore tested the combinatorial effects of these compounds with HSP90 inhibitors on HSP90 client signaling and viability. We found that celastrol and gedunin show mild synergy with geldanamycin and 17-AAG in inhibiting the androgen signaling signature, as shown by isobologram analysis (Figure 5B; Figure S3). Celastrol and gedunin also synergistically inhibit cell growth, assayed by ATP level, with geldanamycin and 17-AAG at low concentrations (Figure 5C; Figure S3). Celastrol and gedunin therefore act synergistically with existing modes of HSP90 ATP-binding site inhibition to inhibit HSP90 client signaling and viability in a cellular context, consistent with their inhibition of HSP90 via a distinct mechanism.

Discussion

Chemical genomics has the potential to identify modulators of complex cancer phenotypes and predict their activities with little prior knowledge about the underlying mechanisms. Here we report a chemical genomic screen for modulators of AR-mediated signaling modulators, a critical cancer signaling pathway. To investigate the activity of the resulting celastrol and gedunin family of hits, a gene expression-based approach was used to identify similar known drug activities and predicted that these compounds act as HSP90 pathway inhibitors. We then validated this hypothesis by demonstrating that celastrol and gedunin destabilize HSP90 clients including AR and inhibit HSP90 function. Moreover, celastrol and gedunin act outside the HSP90 ATP-binding pocket targeted by most HSP90 inhibitors and act synergistically with these inhibitors.

Given the central role that HSP90 and its clients play in cancer biology, celastrol and gedunin compounds represent a significant new set of HSP90 pathway modulators. The work presented here identifies celastrol- and gedunin-mediated inhibition of HSP90 client activity including AR (Yang et al., 2006) and illustrates its broad downstream effects on AR-regulated gene expression (Georget et al., 2002; Waza et al., 2005). Celastrol and gedunin are further shown to affect HSP90 activity and interactions. The decrease in HSP90's ATP-binding activity and HSP90-p23 interaction could result from a shift to the ADP complexed form of HSP90, which directs client proteins to the proteasome (Bali et al., 2005; Felts and Toft, 2003; Soti et al., 2002). Indeed, celastrol treatment is known to cause accumulation of ubiquitinated proteins (Yang et al., 2006); such accumulation can result from HSP90 inhibition and stress response, and the subsequent redirection of proteins through the proteasomal pathway (Mimnaugh et al., 2004). Consistent with HSP90-inhibitory activity, celastrol has also been shown to induce HSP70 levels (Westerheide et al., 2004), a hallmark of HSP90 inhibition by existing ansamycin antibiotic HSP90 inhibitors as well as stress and heat shock response (Murakami et al., 1991). Celastrol has additionally been shown to suppress hERG potassium channel activity by inhibiting hERG maturation (Sun et al., 2006), which is seen with existing HSP90 inhibitors and is hypothesized to result from HSP90 inhibition (Ficker et al., 2003). Both celastrol and existing HSP90 inhibitors appear to be active

in neurodegenerative disease models (Wang et al., 2005; Waza et al., 2005) where, notably, 17-AAG inhibits neurodegeneration induced by polyglutamine expansion of AR. Last, both celastrol and gedunin also have noted antimalarial activity, as have other HSP90 inhibitors (Figueiredo et al., 1998; MacKinnon et al., 1997). These observations can be unified by the present discovery of celastrol and gedunin's HSP90-inhibitory activity.

Celastrol and gedunin compounds have the potential to provide new modes of HSP90 inhibition. Celastrol and gedunin act outside the N-terminal ATP-binding pocket of HSP90 and therefore inhibit HSP90 function by a mechanism that is distinct from that of most existing HSP90 inhibitors. Few compounds inhibit HSP90 through mechanisms outside this N-terminal domain (Bali et al., 2005; Kovacs et al., 2005; Marcu et al., 2000). Only two other existing drugs, cisplatin and novobiocin, act directly on HSP90 outside this fold by binding the C-terminal domain, and even these only induce HSP90 inhibition at high concentrations at which other mechanisms of action likely predominate (Marcu et al., 2000; Whitesell and Lindquist, 2005). While our work demonstrates that celastrol and gedunin inhibit HSP90 function by acting outside the ATP-binding pocket, it remains to be determined whether they act directly or indirectly on HSP90. Induction of heat shock response or other regulatory mechanisms could, for example, indirectly inhibit HSP90 function. Future work may address the mechanistic details of this HSP90 modulation.

Because celastrol and gedunin inhibit HSP90 function through a different mechanism than N-terminal HSP90 inhibitors, celastrol and gedunin compounds may have significant therapeutic and scientific potential. Triterpenoid derivatives of the celastrol and gedunin family compounds may serve as a starting point for development of drugs that prove useful both in combination with existing HSP90 inhibitors or alone, in the advent of resistance against existing inhibitors. Scientifically, celastrol and gedunin may afford further insight into HSP90 biology by providing tools to probe HSP90 function; several significant HSP90 interactors have been discovered through synthetic screens for genes that confer hypersensitivity to geldanamycin-mediated inhibition, for example (Zhao et al., 2005). Thus, celastrol and gedunin offer a unique window into HSP90 inhibition with broad therapeutic and scientific possibilities.

Beyond HSP90 modulation, this work addresses a significant problem in chemical biology: the discovery of modulators of complex cancer phenotypes and the molecular activities underlying these modulators. We have demonstrated a combined chemical genomic approach to compound discovery and characterization based wholly on gene expression. This strategy provides a useful endpoint for drug and activity screening, since assaying associative effects can serve as a proxy for assaying causal effects. Nonetheless, the strength of the gene expression, as opposed to other readouts, as an assay may vary depending on the biology underlying the state being studied.

Significantly, we have applied a robust approach for chemical activity prediction that uses gene expression signature enrichment analysis to identify similar known drug activities. Compendia of gene expression profiles have been previously used to identify gene targets of drug perturbations in both bacteria (Gardner et al., 2003) and yeast (di Bernardo et al., 2005; Hughes et al., 2000; Parsons et al., 2004), but such work has not previously been extended to mammalian systems. The approach presented here identifies a target pathway of two uncharacterized compounds in a manner robust to ad hoc experimental decisions including cell context and treatment parameters. Notably, though some connectivity is dependent upon appropriate context (for example, estrogen signaling requiring estrogen receptor expression), there appears to be cell line independence in the majority of the cases examined (Lamb et al., 2006). One caveat to this approach is that it requires that the activity of query compounds be represented among the profiled drug activities. Our approach additionally may not distinguish between direct and indirect compound activities in all cases, though this may afford a nuanced view. In sum, this work demonstrates a promising chemical genomic strategy for discovering modulators of complex cancer phenotypes and subsequently establishing their mechanisms of action.

Experimental procedures

Reagents and cell lines

Celastrol (Calbiochem) and gedunin (Gaia Chemicals) were solubilized in DMSO. LNCaP.FGC cells (ATCC) were grown in RPMI 1640 (ATCC) with 10% FBS. Ba/F3 cells stably expressing human FLT3, EGFR, and BCR-ABL1 were grown in RPMI 1640, 10% FBS, and 2 ng/ml IL-3. SKBr3 cells were grown in a 1:1 DME:F12 plus 10% FBS.

Gene expression profiling and analysis

The mRNA expression profiles of celastrol- and gedunin-treated cells were determined by Affymetrix U133A microarray analysis in triplicate. RNA was isolated by Trizol extraction from LNCaP cells treated with vehicle, 1.25 μM celastrol, or 20 μM gedunin (1) for 24 hr in RPMI, 10% charcoal-stripped FBS, and 1 nM R1881 or vehicle, following androgen deprivation in charcoal-stripped media for 2 days, and (2) for 6 hr in RPMI with 10% FBS. IVT, labeling, hybridization, and washing were carried out on the Affymetrix High-Throughput Array platform using HT_HG-U133A preproduction arrays (early access version; part number 520276) for all but the 24 hr gedunin samples. U133A version 2 arrays were used for the 24 hr gedunin samples for technical reasons. Raw data were processed by RMA (Table S6). For hierarchical clustering, a 169 probe set of androgen-regulated genes was defined and used to perform average linkage clustering (Supplemental Experimental Procedures). Raw data are available at http://www.broad.mit.edu/cgi-bin/cancer/publications/pub_menu.cgi/ and NCBI's Gene Expression Omnibus (GEO; http://www.ncbi.nlm.nih.gov/geo/; accession numbers GSE5505 to GSE5508).

Gene expression signature analysis

Androgen signaling signature

The androgen signaling signature was developed from independent Affymetrix U133A profiles of LNCaP cells treated with 0.1 nM R1881 over a 24 hr time course (Febbo et al., 2005). Class neighbors analysis was used to identify genes that are differentially expressed upon R1881 androgen treatment relative to vehicle by the SNR metric (Golub et al., 1999; Reich et al., 2006). The top marker genes were tested for differential expression between androgen-stimulated and -deprived states by GE-HTS assay. The 27 genes with the most robust discrimination by SNR were chosen for the GE-HTS androgen signaling signature (Table S3). Two normalization controls, *SRP72* and *KIAA0676*, were selected from genes with moderate expression levels that varied little over the R1881 time course.

Celastrol and gedunin signatures

The celastrol and gedunin signatures were developed from RMA-processed microarray data from LNCaP cells treated with 1.25 μM celastrol or 20 μM gedunin for 6 hr. Comparative marker selection was used to identify markers that distinguished celastrol- and/or gedunin-treated samples from vehicle-treated samples by the median SNR (Golub et al., 1999). The top 50 markers that increased and decreased relative to vehicle-treated controls were used as the signatures (Table S7).

GE-HTS androgen signaling signature assay

The GE-HTS assay was carried out as described (Peck et al., 2006 and Supplemental Data) using AR signature probes (Table S3).

GE-HTS and viability screens

NINDS, Biomol, and SpecPlus libraries (http://www.broad.mit.edu/chembio/platform/screening/compound_libraries/index.htm/) were screened using GE-HTS androgen signaling and viability assays. After 2 days androgen deprivation, LNCaP cells were treated with compounds (~20 μM) or vehicle (DMSO) plus 1 nM R1881 for 24 hr for the GE-HTS screen and for 3 days for the viability screen. Raw GE-HTS expression levels were filtered and normalized (Table S8) as described in the Supplemental Experimental Procedures. Compounds were scored by weighted and unweighted "summed score" metrics, KNN classifier, and naive Bayes classifier to identify candidate modulators that induced the androgen deprivation signature (Supplemental Experimental Procedures). For heat map visualization, screen data were normalized between libraries using the mean SRP72 value of the androgen-deprived vehicle controls (Table S9).

Viability and soft agar assays

Adherent cell growth was measured by luminescent assay of ATP level (CellTiterGlo, Promega). LNCaP cells were grown in charcoal-stripped media for 2 days prior to simultaneous treatment with 1 nM R1881 and the relevant compound. Synergy was assessed by analyzing the IC50 of one drug over a range of concentrations of the other drug and vice versa. The resulting concentration pairs were visualized by isobologram (Gessner, 1995). Anchorage independence was measured by soft agar assay (Hahn et al., 1999). Compounds were added to both agar layers. Colonies were scored after 3 weeks.

Connectivity Map analysis for drug activity

The current version of the Connectivity Map data set (build01) contains genome-wide expression data for 453 treatment and vehicle control pairs, representing 164 distinct small molecules. Cell treatments and Affymetrix profiling were predominantly carried out in MCF7 cells with 6 hr treatments as detailed (Table S4) (Lamb et al., 2006). Enrichment of the induced and repressed genes of a signature within each Connectivity Map treatment profile was estimated with a metric based on the Kolmogorov-Smirnov statistic as described (Lamb et al., 2003, 2006). Connectivity Map data are available at http://www.broad.mit.edu/cmap/ and GEO (accession number GSE5258).

Western blotting

Western blotting was carried out as described (Ebert et al., 2005). The following antibodies were used: AR N-20 (1:250, sc-816, Santa Cruz), EGFR (1:1000, CST2232, Cell Signaling), ABL (1:1000, CST2862, Cell Signaling), phospho-tyrosine 4G10 for P-BCR-ABL1 (05-321, Upstate), FLT3/FLK2 S-18 (1:1000, sc-480, Santa Cruz), HSP90α (1:250, Stressgen, SPS-771F), HSP90 (1:5000, Abcam), CSK H-75 (1:250, Santa Cruz, sc-13074x), DDR1 H-126 (1:250, Santa Cruz, sc-8988x), hHSP90 H9010, Hop F5, and p23 JJ3, tubulin (1:5000, Abcam, ab6046), and actin (1:5000, Abcam, ab8227-50).

HSP90 ATP-binding assay

The ATP-binding assay was similar to that in previous reports (Bali et al., 2005; Soti et al., 2002). LNCaP and K562 cells were treated with celastrol and gedunin for 24 hr and then lysed in TNESV buffer (50 mM Tris, 2 mM EDTA, 100 nM NaCl, 1 mM activated sodium orthovanadate, 25 mM NaF, 1% Triton X-100 [pH 7.5]) for 30 min at 4°C. Lysates were spun for 30 min at 12,000 rpm at 4°C. Protein (200 μg) was incubated with conditioned γ-ATP-polyacrylamide resin (Novagen) in incubation buffer (10 mM Tris-HCl, 50 mM KCl, 5 mM $MgCl_2$, 20 mM Na_2MoO_4, 0.01% Nonidet P-40) overnight at 4°C, rotating. The resin was then washed four times with incubation buffer. Bound proteins were isolated by boiling with SDS buffer.

HSP90 coimmunoprecipitation

SKBR-3 cells were treated with vehicle, celastrol (2.5 μM, 12 hr), and PU24FCl (20 μM, 24 hr) (Vilenchik et al., 2004). Cells were lysed in 20 mM Tris HCl (pH 7.4), 25 mM NaCl, 2 mM DDT, 20 mM Na_2MoO4, 0.1% NP-40, and protein inhibitors. Lysates were incubated for 2 hr at 4°C, rotating, and then centrifuged at 13,000 × g for 10 min. Protein (500 μg) was incubated with H9010 anti-HSP90 antibody for 1 hr at 4°C, rotating. Protein G agarose (30 μl; Upstate) was added to each sample, and samples were then incubated for 1 hr at 4°C, rotating. The beads were washed five times with 1 ml lysis buffer. Bound proteins were isolated by boiling in sample buffer. The levels of HSP90 and coimmunoprecipitating proteins were analyzed by western blot.

Geldanamycin competition assay

The geldanamycin competition assay was performed as described (He et al., 2006; Kim et al., 2004), except that Cy3B-geldanamycin rather than BODIPY-geldanamycin was used (Supplemental Experimental Procedures).

Supplemental data

The Supplemental Data include Supplemental Experimental Procedures, nine supplemental tables, and three supplemental figures and can be found with this article online at http://www.cancercell.org/cgi/content/full/10/4/321/DC1/.

Acknowledgments

We thank Jane Jiang, James Griffin, Azam Mohammad, and George Daley for Ba/F3 cell lines and Phil Febbo for use of microarray data from androgen-stimulated and -deprived LNCaP cells. hHSP90 H9010, Hop F5, and p23 JJ3 antibodies were a generous gift from David O. Toft. This work was supported by a Damon Runyon fellowship to H.H. and NIH and HHMI grants to T.R.G. In compliance with HMS guidelines, we disclose that W.C.H. is a consultant for Novartis Pharmaceuticals, Inc.

Received: June 15, 2006
Revised: August 30, 2006
Accepted: September 13, 2006
Published online: September 28, 2006

References

Bagatell, R., Beliakoff, J., David, C.L., Marron, M.T., and Whitesell, L. (2005). Hsp90 inhibitors deplete key anti-apoptotic proteins in pediatric solid tumor cells and demonstrate synergistic anticancer activity with cisplatin. Int. J. Cancer *113*, 179–188.

Bali, P., Pranpat, M., Bradner, J., Balasis, M., Fiskus, W., Guo, F., Rocha, K., Kumaraswamy, S., Boyapalle, S., Atadja, P., et al. (2005). Inhibition of histone deacetylase 6 acetylates and disrupts the chaperone function of heat shock protein 90: A novel basis for antileukemia activity of histone deacetylase inhibitors. J. Biol. Chem. *280*, 26729–26734.

Chen, C.D., Welsbie, D.S., Tran, C., Baek, S.H., Chen, R., Vessella, R., Rosenfeld, M.G., and Sawyers, C.L. (2004). Molecular determinants of resistance to antiandrogen therapy. Nat. Med. *10*, 33–39.

di Bernardo, D., Thompson, M.J., Gardner, T.S., Chobot, S.E., Eastwood, E.L., Wojtovich, A.P., Elliott, S.J., Schaus, S.E., and Collins, J.J. (2005). Chemogenomic profiling on a genome-wide scale using reverse-engineered gene networks. Nat. Biotechnol. *23*, 377–383.

Ebert, B.L., Lee, M.M., Pretz, J.L., Subramanian, A., Mak, R., Golub, T.R., and Sieff, C.A. (2005). An RNA interference model of RPS19 deficiency in Diamond-Blackfan anemia recapitulates defective hematopoiesis and rescue by dexamethasone: Identification of dexamethasone-responsive genes by microarray. Blood *105*, 4620–4626.

Febbo, P.G., Lowenberg, M., Thorner, A.R., Brown, M., Loda, M., and Golub, T.R. (2005). Androgen mediated regulation and functional implications of fkbp51 expression in prostate cancer. J. Urol. *173*, 1772–1777.

Feldman, B.J., and Feldman, D. (2001). The development of androgen-independent prostate cancer. Nat. Rev. Cancer *1*, 34–45.

Felts, S.J., and Toft, D.O. (2003). p23, a simple protein with complex activities. Cell Stress Chaperones *8*, 108–113.

Ficker, E., Dennis, A.T., Wang, L., and Brown, A.M. (2003). Role of the cytosolic chaperones Hsp70 and Hsp90 in maturation of the cardiac potassium channel HERG. Circ. Res. *92*, e87–e100.

Figueiredo, J.N., Raz, B., and Sequin, U. (1998). Novel quinone methides from Salacia kraussii with in vitro antimalarial activity. J. Nat. Prod. *61*, 718–723.

Gardner, T.S., di Bernardo, D., Lorenz, D., and Collins, J.J. (2003). Inferring genetic networks and identifying compound mode of action via expression profiling. Science *301*, 102–105.

Georget, V., Terouanne, B., Nicolas, J.C., and Sultan, C. (2002). Mechanism of antiandrogen action: Key role of hsp90 in conformational change and transcriptional activity of the androgen receptor. Biochemistry *41*, 11824–11831.

Gessner, P.K. (1995). Isobolographic analysis of interactions: An update on applications and utility. Toxicology *105*, 161–179.

Golub, T.R., Slonim, D.K., Tamayo, P., Huard, C., Gaasenbeek, M., Mesirov, J.P., Coller, H., Loh, M.L., Downing, J.R., Caligiuri, M.A., et al. (1999). Molecular classification of cancer: Class discovery and class prediction by gene expression monitoring. Science *286*, 531–537.

Hahn, W.C., Counter, C.M., Lundberg, A.S., Beijersbergen, R.L., Brooks, M.W., and Weinberg, R.A. (1999). Creation of human tumour cells with defined genetic elements. Nature *400*, 464–468.

He, H., Zatorska, D., Kim, J., Aguirre, J., Llauger, L., She, Y., Wu, N., Immormino, R.M., Gewirth, D.T., and Chiosis, G. (2006). Identification of potent water soluble purine-scaffold inhibitors of the heat shock protein 90. J. Med. Chem. *49*, 381–390.

Holzbeierlein, J., Lal, P., LaTulippe, E., Smith, A., Satagopan, J., Zhang, L., Ryan, C., Smith, S., Scher, H., Scardino, P., et al. (2004). Gene expression analysis of human prostate carcinoma during hormonal therapy identifies androgen-responsive genes and mechanisms of therapy resistance. Am. J. Pathol. *164*, 217–227.

Hughes, T.R., Marton, M.J., Jones, A.R., Roberts, C.J., Stoughton, R., Armour, C.D., Bennett, H.A., Coffey, E., Dai, H., He, Y.D., et al. (2000). Functional discovery via a compendium of expression profiles. Cell *102*, 109–126.

Kim, J., Felts, S., Llauger, L., He, H., Huezo, H., Rosen, N., and Chiosis, G. (2004). Development of a fluorescence polarization assay for the molecular chaperone Hsp90. J. Biomol. Screen. *9*, 375–381.

Kovacs, J.J., Murphy, P.J., Gaillard, S., Zhao, X., Wu, J.T., Nicchitta, C.V., Yoshida, M., Toft, D.O., Pratt, W.B., and Yao, T.P. (2005). HDAC6 regulates Hsp90 acetylation and chaperone-dependent activation of glucocorticoid receptor. Mol. Cell *18*, 601–607.

Lam, J.S., Leppert, J.T., Vemulapalli, S.N., Shvarts, O., and Belldegrun, A.S. (2006). Secondary hormonal therapy for advanced prostate cancer. J. Urol. *175*, 27–34.

Lamb, J., Ramaswamy, S., Ford, H.L., Contreras, B., Martinez, R.V., Kittrell, F.S., Zahnow, C.A., Patterson, N., Golub, T.R., and Ewen, M.E. (2003). A mechanism of cyclin D1 action encoded in the patterns of gene expression in human cancer. Cell *114*, 323–334.

Lamb, J., Crawford, E.D., Peck, D., Modell, J.W., Blat, I.C., Wrobel, M.J., Lerner, J., Brunet, J.-P., Subramanian, A., Ross, K.N., et al. (2006). The connectivity map: Using gene-expression signatures to connect small molecules, genes and disease. Science, in press.

Linja, M.J., Savinainen, K.J., Saramaki, O.R., Tammela, T.L., Vessella, R.L., and Visakorpi, T. (2001). Amplification and overexpression of androgen receptor gene in hormone-refractory prostate cancer. Cancer Res. *61*, 3550–3555.

Llauger-Bufi, L., Felts, S.J., Huezo, H., Rosen, N., and Chiosis, G. (2003). Synthesis of novel fluorescent probes for the molecular chaperone Hsp90. Bioorg. Med. Chem. Lett. *13*, 3975–3978.

MacKinnon, S., Durst, T., Arnason, J.T., Angerhofer, C., Pezzuto, J., Sanchez-Vindas, P.E., Poveda, L.J., and Gbeassor, M. (1997). Antimalarial activity of tropical Meliaceae extracts and gedunin derivatives. J. Nat. Prod. *60*, 336–341.

Majumder, P.K., and Sellers, W.R. (2005). Akt-regulated pathways in prostate cancer. Oncogene *24*, 7465–7474.

Marcu, M.G., Schulte, T.W., and Neckers, L. (2000). Novobiocin and related coumarins and depletion of heat shock protein 90-dependent signaling proteins. J. Natl. Cancer Inst. *92*, 242–248.

Mimnaugh, E.G., Xu, W., Vos, M., Yuan, X., Isaacs, J.S., Bisht, K.S., Gius, D., and Neckers, L. (2004). Simultaneous inhibition of hsp 90 and the proteasome promotes protein ubiquitination, causes endoplasmic reticulum-derived cytosolic vacuolization, and enhances antitumor activity. Mol. Cancer Ther. *3*, 551–566.

Murakami, Y., Uehara, Y., Yamamoto, C., Fukazawa, H., and Mizuno, S. (1991). Induction of hsp 72/73 by herbimycin A, an inhibitor of transformation by tyrosine kinase oncogenes. Exp. Cell Res. *195*, 338–344.

Padma, T.V. (2005). Ayurveda. Nature *436*, 486.

Parsons, A.B., Brost, R.L., Ding, H., Li, Z., Zhang, C., Sheikh, B., Brown, G.W., Kane, P.M., Hughes, T.R., and Boone, C. (2004). Integration of chemical-genetic and genetic interaction data links bioactive compounds to cellular target pathways. Nat. Biotechnol. *22*, 62–69.

Peck, D., Crawford, E.D., Ross, K.N., Stegmaier, K., Golub, T.R., and Lamb, J. (2006). A method for high-throughput gene expression signature analysis. Genome Biol. *7*, R61.

Reich, M., Liefeld, T., Gould, J., Lerner, J., Tamayo, P., and Mesirov, J.P. (2006). GenePattern 2.0. Nat. Genet. *38*, 500–501.

Soti, C., Racz, A., and Csermely, P. (2002). A nucleotide-dependent molecular switch controls ATP binding at the C-terminal domain of Hsp90. N-terminal nucleotide binding unmasks a C-terminal binding pocket. J. Biol. Chem. *277*, 7066–7075.

Stegmaier, K., Ross, K.N., Colavito, S.A., O'Malley, S., Stockwell, B.R., and Golub, T.R. (2004). Gene expression-based high-throughput screening (GE-HTS) and application to leukemia differentiation. Nat. Genet. *36*, 257–263.

Sun, H., Liu, X., Xiong, Q., Shikano, S., and Li, M. (2006). Chronic inhibition of cardiac kir2.1 and HERG potassium channels by celastrol with dual effects on both ion conductivity and protein trafficking. J. Biol. Chem. *281*, 5877–5884.

Ushiro, S., Ono, M., Nakayama, J., Fujiwara, T., Komatsu, Y., Sugimachi, K., and Kuwano, M. (1997). New nortriterpenoid isolated from anti-rheumatoid arthritic plant, Tripterygium wilfordii, modulates tumor growth and neovascularization. Int. J. Cancer *72*, 657–663.

Vilenchik, M., Solit, D., Basso, A., Huezo, H., Lucas, B., He, H., Rosen, N., Spampinato, C., Modrich, P., and Chiosis, G. (2004). Targeting wide-range oncogenic transformation via PU24FCl, a specific inhibitor of tumor Hsp90. Chem. Biol. *11*, 787–797.

Visakorpi, T., Hyytinen, E., Koivisto, P., Tanner, M., Keinanen, R., Palmberg, C., Palotie, A., Tammela, T., Isola, J., and Kallioniemi, O.P. (1995). In vivo amplification of the androgen receptor gene and progression of human prostate cancer. Nat. Genet. *9*, 401–406.

Walsh, P.C. (1996). Treatment of benign prostatic hyperplasia. N. Engl. J. Med. *335*, 586–587.

Wang, J., Gines, S., MacDonald, M.E., and Gusella, J.F. (2005). Reversal of a full-length mutant huntingtin neuronal cell phenotype by chemical inhibitors of polyglutamine-mediated aggregation. BMC Neurosci. *6*, 1.

Waza, M., Adachi, H., Katsuno, M., Minamiyama, M., Sang, C., Tanaka, F., Inukai, A., Doyu, M., and Sobue, G. (2005). 17-AAG, an Hsp90 inhibitor, ameliorates polyglutamine-mediated motor neuron degeneration. Nat. Med. *11*, 1088–1095.

Westerheide, S.D., Bosman, J.D., Mbadugha, B.N., Kawahara, T.L., Matsumoto, G., Kim, S., Gu, W., Devlin, J.P., Silverman, R.B., and Morimoto, R.I. (2004). Celastrols as inducers of the heat shock response and cytoprotection. J. Biol. Chem. *279*, 56053–56060.

Whitesell, L., and Lindquist, S.L. (2005). HSP90 and the chaperoning of cancer. Nat. Rev. Cancer *5*, 761–772.

Yang, H., Chen, D., Cui, Q.C., Yuan, X., and Dou, Q.P. (2006). Celastrol, a triterpene extracted from the Chinese "Thunder of God Vine," is a potent proteasome inhibitor and suppresses human prostate cancer growth in nude mice. Cancer Res. *66*, 4758–4765.

Zhao, R., Davey, M., Hsu, Y.C., Kaplanek, P., Tong, A., Parsons, A.B., Krogan, N., Cagney, G., Mai, D., Greenblatt, J., et al. (2005). Navigating the chaperone network: An integrative map of physical and genetic interactions mediated by the hsp90 chaperone. Cell *120*, 715–727.

Accession numbers

The Affymetrix data presented here are available from NCBI's Gene Expression Omnibus as series GSE5505 to GSE5508 (LNCaP data) and GSE5258 (Connectivity Map).